D-27

LAND SURFACE DEFORMATION MEASUREMENT BY SAR INTERFEROMETRY USING L-BAND AND C-BAND DATA SETS

Yusupujiang Aimaiti, Wen Liu, and Fumio Yamazaki

Chiba University, Chiba 263-8522, Japan Email:tuprak100@gmail.com

ABSTRACT: Synthetic Aperture Radar (SAR) interferometry is a technique that provides high-resolution measurements of the ground displacement associated with many geophysical processes. In our previous work, in order to investigate the land surface deformation in Karamay, a typical oil-producing city in Xinjiang Uyghur Autonomous Region, China, ALOS PALSAR L-band data acquired in the period of 2007-2009 were used for the two-pass differential SAR interferometry (D-InSAR) process. The experimental results showed that two sites in the north-eastern part of the city exhibit clear indication of land deformation. For further evaluating the result of D-InSAR processing, the PS and SBAS-InSAR techniques were applied for 21 time-series ENVISAT ASAR C-band data sets in 2003-2010. The final results showed that the results from the D-InSAR and SBAS-InSAR measurements had better agreement than that from the PS-InSAR measurement. This may be related to the fact that the study area was mostly non-urban land-use, which is difficult to find enough persistent scatter points with sufficiently high coherence in the processing.

KEY WORDS: ALOS PALSAR, ENVISAT ASAR, Deformation, D-InSAR, PS-InSAR, SBAS-InSAR

1. INTRODUCTION

Karamay, which means "black oil" in Uyghur language, is a typical mining city, relying on oil field exploration and development. It has abundant deposits of heavy and ultra-heavy oil that are estimated to be several hundred million tons (Yuan et al, 2013). After several years of oil field development, a subsurface water injection project was initiated in 1985 to increase the effectiveness of oil recovery (Li et al., 2011). In most case, the oil and gas extraction from underground reservoirs and waste-water injection induce deformation in reservoirs by changing the reservoir pressure and consequently generates measurable surface deformations as subsidence or uplift (Khakim et al., 2012).

While there is a lack of ground-based measurements, the advanced remote sensing technologies, especially the Interferometric Synthetic Aperture Radar (InSAR) can be a powerful tool for remotely mapping the human and nature-induced ground deformation (Liu et al., 2015; Schmidt & Bürgmann, 2003; Heimlich et al., 2015). Recently Shirzaei et al. (2016) used the multi-temporal InSAR approach and revealed the relationship between the wastewater injection in different depths with surface uplift and time-dependent seismic hazard at the oil well sites in the eastern Texas, USA.

In our previous work, for better understanding the land surface deformation in Karamay oil field, two path D-InSAR method was applied to three L-band SAR images acquired by ALOS PALSAR over the study area in the period from January 20, 2007 to January 25 2009 (Aimaiti et al., 2016). To validate the results obtained by ALOS observations, we further applied the Persistent Scatter (PS) and Small baseline subset (SBAS)-InSAR technique to 21 C-band images acquired by the ENVISAT ASAR in the period from 30 September 2003 to 15 June 2010.

2. STUDY AREA AND DATA SETS

2.1 The study area

Karamay city is a prefecture-level city in the north of the Xinjiang Uyghur Autonomous Region, the People's Republic of China. There are four administrative districts in Karamay, which are Urho, Baijiantan, Karamay and Dushanzi with a total area of 9,500 km^2. The Karamay oil field in Xinjiang is the largest oil field in China. The geomorphological type of Karamay is predominantly Gobi desert. The altitude is in the range between 250 m and 500 m.

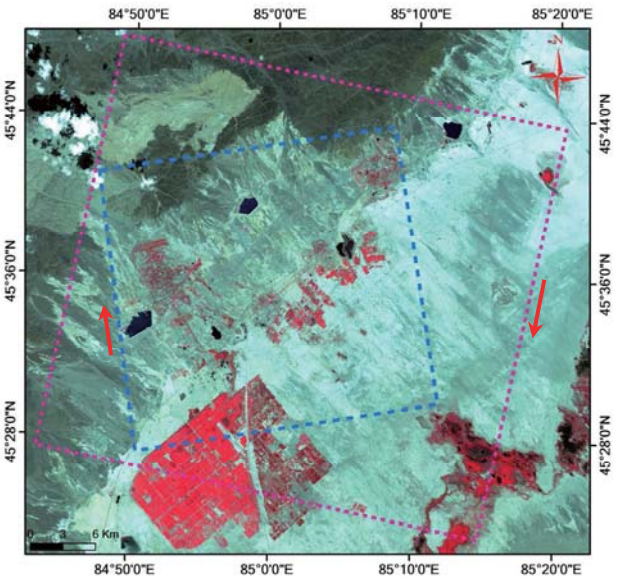

Figure 1. Geographic location of study area
(Note: Blue and pink lines are indicating the coverage area of ALOS-PALSAR and ENVISAT-ASAR data, respectively).

2.2 Data sets

In the previous study, the ALOS PALSAR data sets covering the region of interest were provided by the Japan Space Exploration Agency (JAXA). The SAR interferograms were computed from PALSAR fine-beam single-polarization (FBS) data taken on three different dates (January 20, 2007, December 10, 2008, and January 25, 2009). The data sets have the same observation parameters: the reference system for planning (RSP) number 94, the path number 501, and acquired from the ascending orbit with an off-nadir angle of 34.3°. We also used twenty-one C-band ENVISAT ASAR images acquired in the period from Sep. 30, 2003 to June 15, 2010, provided by the European Space Agency (ESA). The data sets were acquired on the descending orbit with an incidence angle of 22.9°. A subset area was selected from the original images corresponding to the whole study area. The cover ranges of the ALOS and ENVISAT data are shown in Figure 1.

3. METHODS

3.1 D-InSAR

In this study, the two-pass Interfrometry method was implemented using two ALOS PALSAR SLC images for interferogram generation. Then the topographic phase in the wrapped phase was removed by introducing SRTM DEM data. To reduce noises and smooth the interferogram, the Goldstein–Werner filtering process was applied. Finally the InSAR products were geocoded from the Range-Doppler coordinates to the map geometry corresponding of the Universal Transverse Mercator (UTM) projection (zone 45N) with a pixel resolution of 25 m. ENVI and SARscape software were employed to process the level-1.1 data and perform the interferometric analysis.

3.2 PS and SBAS-InSAR

The PS-InSAR is one of the promising approach that improves the precision of conventional InSAR displacement measurements. The PS-InSAR algorithm utilizes time series of radar images to detect coherent radar signals from PS points in order to derive information of terrain motion (Ferretti et al., 2001). Another algorithm called small baseline subset (SBAS), which use conventional interferograms with small baselines to obtain time-series displacements (Berardino et al., 2002). The both algorithms work to minimize the disadvantages of conventional D-InSAR, namely the phase errors due to the geometrical and temporal decorrelations as well as the atmospheric disturbance.

The ENVISAT-ASAR data were processed using both PS-InSAR and SBAS-InSAR methods. For the PS-InSAR, we selected the slant range image on November 28, 2006, as the master image and generated 20 interferograms with respect to the master image. The time position plot is shown in Figure 2. For the SBAS-InSAR, we selected the slant range image on October 28, 2008, as the super master image, and generated 68 interferograms using a maximum temporal baseline of 735 days and a maximum spatial baseline of 483 m. The time position plot is shown in Figure 3.

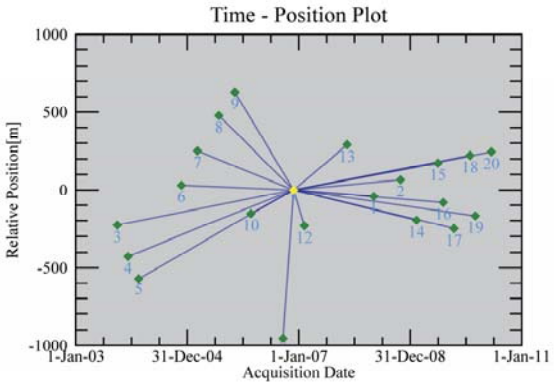

Figure 2. Time position plot for the PS-InSAR

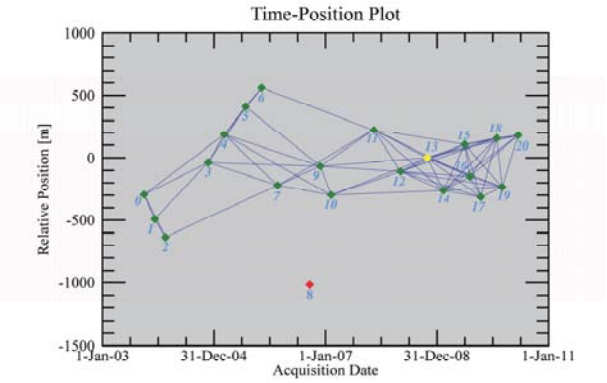

Figure 3. Time position plot for the SBAS-InSAR

4. RESULTS AND ANALYSIS

4.1 Results of D-InSAR interferometry

For the D-InSAR generation, we have two data pairs (2007/01/20 & 2008/12/10, Bn = 643m; 2008/12/10 & 2009/1/25, Bn = 472m). Although the interferogram with a relatively small normal baseline showed good coherence, no significant land deformation was found. It is due to the short period of time, 46 days. Therefore, we used the differential interferogram generated from the large normal baseline pair, which showed clear deformation at two sites in the study area. These areas were indicated by blue dashed circles in Figure 4. In the process of extracting the ground displacement, we unwrapped the interferogram in order to solve the 2π ambiguity and corrected the satellite orbit inaccuracies and phase offset using the collected external ground control points (GCPs). The final ground displacement map in the slant-range direction is shown in Figure 5. From the figure, we could see that two sites in the north-eastern part of the city exhibit clear indications of land uplift. The maximum displacement was 12.97 cm in the study period.

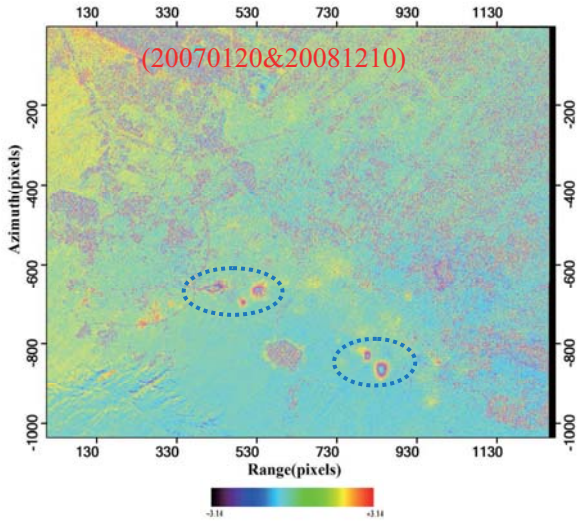

Figure 4. D-InSAR interferogram obtained from the ALOS PALSAR images taken on Jan. 20, 2007 and Dec. 10, 2008.

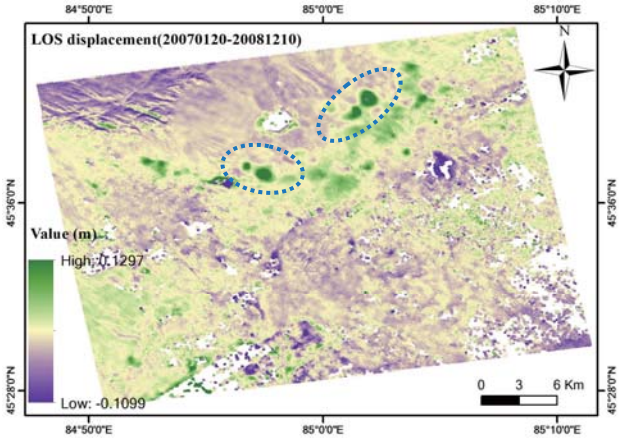

Figure 5. Displacements in the slant-range direction obtained by the D-InSAR analysis from the ALOS PALSAR pair.

4.2 Results of PS and SBAS-InSAR interferometry

The PS-InSAR and SBAS-InSAR analyses were carried out using the ENVISAT-ASAR dataset. The results showed significant surface deformation over or near the oil field working area (Figures 6 and 7). Figure 6 represents the spatial density of PS points and also reveals the spatial distribution of the mean deformation velocity (mm/year) from 2003 to 2010, where the main deformation areas are indicated in blue dashed circles. Temporal decorrelation due to the large amount of the agricultural areas was excluded based on the coherence value larger than 0.65. Dense PS points were detected around the reservoir area, whereas the distribution of PS points were sparse in other areas. The maximum rate of deformation was about 24.4 mm/year.

The locations and the average surface displacement velocity detected by the SBAS-InSAR technique in the study area are shown in Figure 7. It could be seen that two significant land uplift locations were detected in this study area, which were indicated in blue dashed circles. They are located around the oil production wells. The maximum deformation velocity was about 33.3 mm/year.

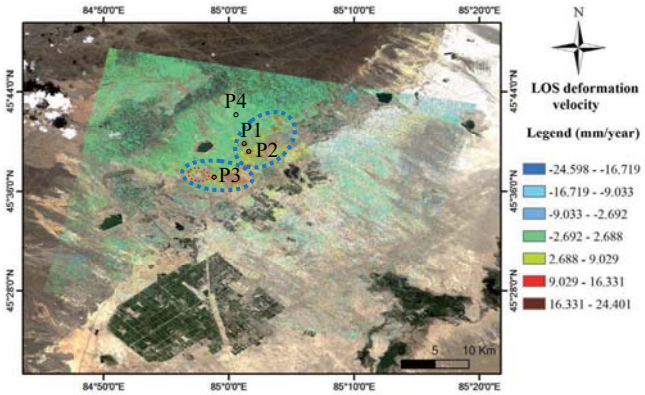

Figure 6. Estimated mean displacement velocity using the PS-InSAR method from the ENVISAR-ASAR dataset.

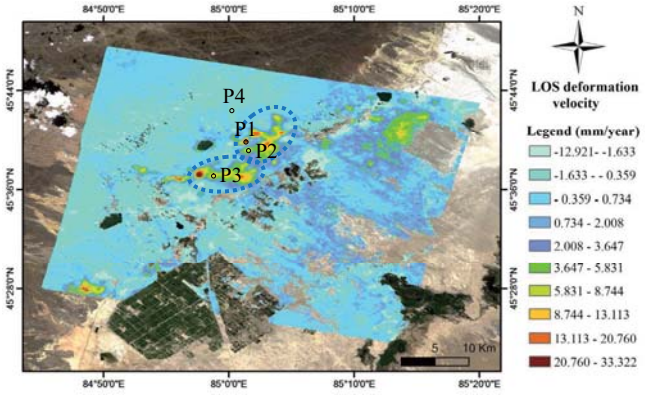

Figure 7. Estimated mean displacement velocity using the SBAS-InSAR method from the ENVISAR-ASAR dataset.

4.3 Time series analysis of PS and SBAS-InSAR

Figure 8 shows the displacement rate distribution between PS-InSAR and SBAS-InSAR time series measurements (from 2003/09/30 to 2010/06/15) in the Karamay oil field. We selected three typical reference points with the induced deformation as the P1-P3 in Figures 6 and 7, and one stable reference point as the P4. Figure 8 illustrates that the both PS-InSAR and SBAS-InSAR methods have good agreement in the deformation trend, which is the increasing uplift.

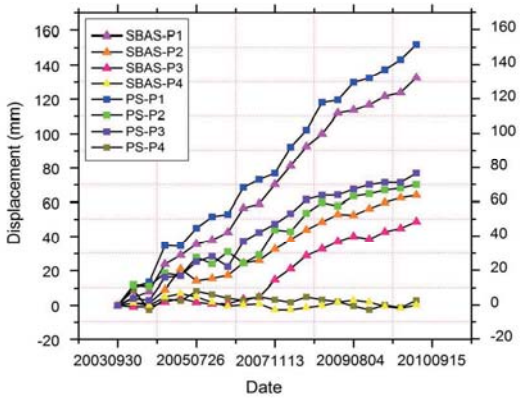

Figure 8. Time-series of the line-of-sight displacements obtained by the PS-InSAR and SBAS-InSAR methods at the locations, P1-P4

4.4 Comparison of the results from D-InSAR, PS and SBAS-InSAR methods

In order to compare the deformation results obtained from the D-InSAR, PS and SBAS-InSAR methods, the mean deformation velocity of D-InSAR processing results was calculated by averaging the displacement values. We selected 500 reference points from the PS-InSAR results in the study area, include both the stable and deformed areas. The LOS displacements velocity for these points was plotted comparing with the SBAS and D-InSAR results, and the correlation coefficients were calculated. The results showed good agreement between SBAS and D-InSAR methods with the correlation of 0.76. However, the correlation between D-InSAR and PS-InSAR was not so good match with a low correlation of 0.54. All of the three methods have identified the main deformation areas, except one of the main deformation areas in PS-InSAR indicated in red dashed circles in Figure 6. It may be caused by low backscatter in the wide non-urban land use, where the sufficient number of PS points could not be collected in the PS-In SAR processing.

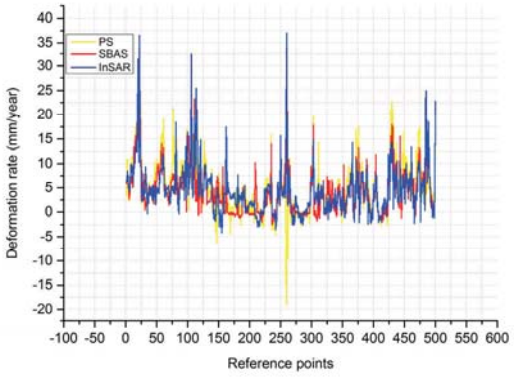

Figure 9 Comparison of D-InSAR, PS and SBAS-InSAR results

5. CONCLUSION

In order to address oil field deformation in Karamay, Xinjiang, China, the D-InSAR technique was applied to ALOS PALSAR data and the PS-InSAR and SBAS-InSAR to ENVISAT ASAR dataset. The results showed that these techniques can provide useful information for identifying the boundaries of deformation and monitoring the temporal behaviour of land deformation. The three methods revealed two areas of land uplift near the oil field. The maximum deformation velocity was estimated to be 33.3 mm/year. The subsurface water injection to enhanced oil recovery might be responsible for the land uplift. The comparison of the obtained results from the three methods indicated that the correlation of the SBAS-InSAR and D-InSAR results is higher than that of the PS-InSAR and D-InSAR results. For this study area, the SBAS-InSAR seems to be more robust than the PS-InSAR. The future work will be focused on the GPS base station establishment in the high deformation area and monitoring of long time period land deformation by integrating other data.

Acknowledgements

We would like to thank JAXA for providing ALOS-PALSAR data and ESA for providing the ENVISAT-ASAR data used in this study.

References

Aimaiti, Y., Kasimu, A., Maimaitiyiming, Y., 2016. Detection of land subsidence in the area of intensive oil production by ALOS PALSAR data. *IEEE International Geoscience and Remote Sensing Symposium*, 4956-4959.

Berardino, P., Fornaro, G., Lanari, R., Sansosti, E. 2002. A new algorithm for surface deformation monitoring based on small baseline differential interferograms. *IEEE Transactions on Geoscience and Remote Sensing*, 40(11), 2375–2383.

Ferretti, A., Prati, C., Rocca, F. 2001. Permanent scatterers in SAR interferometry. *IEEE Transactions on Geoscience and Remote Sensing*, 39, 8–20.

Heimlich, C., Gourmelen, N., Masson, F., Schmittbuhl, J., Kim, S. W., & Azzola, J. 2015. Uplift around the geothermal power plant of Landau (Germany) as observed by InSAR monitoring. *Geothermal Energy*, 3(1), 2.

Khakim M.Y.N., Tsuji T, Matsuoka T. 2012. Geomechanical modeling for InSAR-derived surface deformation at steam-injection oil sand fields. *Journal of Petroleum Science and Engineering*, 96, 152-161.

Liu, W., Yamazaki, F., Matsuoka, M., Nonaka, T., Sasagawa, T. 2015. Estimation of three-dimensional crustal movements in the 2011 Tohoku-Oki, Japan, earthquake from TerraSAR-X intensity images. *Natural Hazards and Earth System Sciences*, 15(3), 637-645.

Li, X., W. Li, B. Gao, and D. Yang. 2012. Study on Subsurface Water Injection in Qizhong Area of Karamay Oilfield. *Xinjiang Oil & Gas*, 8 (3): 57–59 (in Chinese].

Schmidt, DA, Bürgmann, R. 2003. Time−dependent land uplift and subsidence in the Santa Clara valley, California, from a large interferometric synthetic aperture radar data set. *Journal of Geophysical Research: Solid Earth*, 108 (B9).

Shirzaei, M., Ellsworth, W. L., Tiampo, K. F., González, P. J., Manga, M. 2016. Surface uplift and time-dependent seismic hazard due to fluid injection in eastern Texas. *Science*, 353 (6306), 1416-1419.

Yuan Y, Dou S, Zhang J, Chen S, Xu B. 2013. Consideration of geomechanics for in situ bitumen recovery in Xinjiang, China, S*PE heavy oil conference-Canada*, SPE 165414.